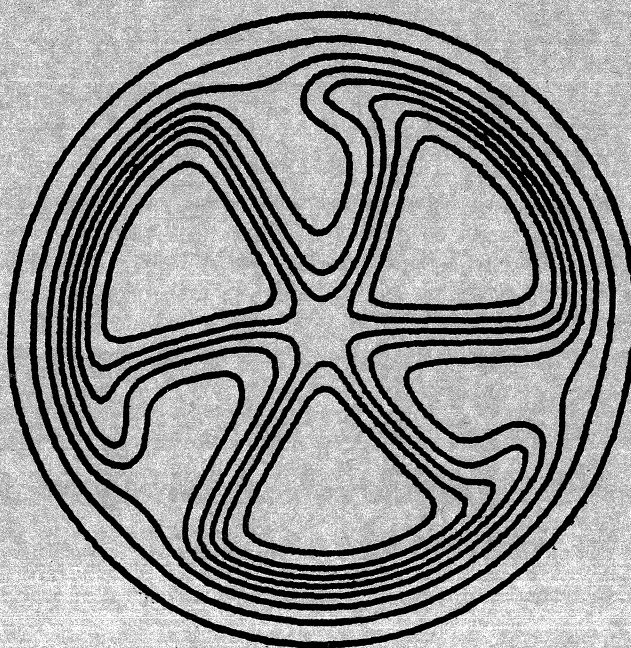


MICHIGAN STATE UNIVERSITY

CYCLOTRON LABORATORY

A MICROSCOPIC INTERPRETATION OF INELASTIC  
PROTON SCATTERING FROM  $^{138}\text{Ba}$  AND  $^{144}\text{Sm}$

DUANE LARSON, SAM M. AUSTIN and B.H. WILDENTHAL





## I. INTRODUCTION

A MICROSCOPIC INTERPRETATION OF INELASTIC  
 PROTON SCATTERING FROM  $^{138}\text{Ba}$  and  $^{144}\text{Sm}$  \*

Duane Larson, † Sam M. Austin and B. H. Wildenthal  
 Cyclotron Laboratory and Department of Physics  
 Michigan State University, East Lansing, Michigan 48824

## ABSTRACT

Microscopic DWBA calculations for the  $(p,p')$  reaction at  $E_p = 30$  MeV have been performed for  $2^+$ ,  $4^+$ , and  $6^+$  states in  $^{138}\text{Ba}$  and  $^{144}\text{Sm}$ . Large-basis shell-model wave functions were used to describe the nuclear states. The effective two-body interaction mediating the inelastic scattering was obtained from a recent survey of inelastic scattering analyses. Polarization charges for the nucleons were extracted using a scheme based on the model of Atkinson and Madsen. Two sets of shell-model wave functions were employed for the  $^{138}\text{Ba}$  calculation, and it was found that comparison of the inelastic proton scattering calculations with experiment clearly distinguished between the two sets. For the better wave functions, the polarization charges were essentially independent of state and multipole.

NUCLEAR REACTIONS  $^{138}\text{Ba}(p,p')$ ,  $^{138}\text{Ba}$ ,  $^{144}\text{Sm}(p,p')$ ,  $^{144}\text{Sm}$ ,  
 30 MeV; calculated  $\sigma(\theta)$ ; deduced  
 polarization charges.

\* Research supported by the National Science Foundation.

† Present address: Neutron Physics Division, Oak Ridge National Laboratory, Oak Ridge, Tennessee.

The nuclei which concern us in this paper are  $^{138}\text{Ba}$  and  $^{144}\text{Sm}$ . These are so-called "N=82" nuclei, consisting of 6 and 12 valence protons, respectively, outside an assumed closed N=82, Z=50 core. We have measured the angular distributions for inelastic scattering of 30 MeV protons to about fifteen low-lying states in each of these nuclei. The results of that experiment, along with a discussion of other properties of these nuclei, are found in Ref. 1. In this paper we analyze the inelastic scattering to the first and second  $2^+$ ,  $4^+$ , and  $6^+$  states in  $^{138}\text{Ba}$  and  $^{144}\text{Sm}$  using shell-model wave functions to describe the states and a realistic effective two-body force, taken from a recent survey<sup>2</sup> of inelastic scattering data, to describe the interaction between the incident proton and the valence protons in the target. The knock-on exchange term is included exactly, an important point since recent microscopic analyses of inelastic nuclear scattering data<sup>3-6</sup> have shown that inclusion of the knock-on exchange amplitude removes many of the inconsistencies found in earlier comparisons of experiment and theory.<sup>7</sup>

Most previous microscopic DWBA calculations for inelastic scattering have been restricted to regions of the periodic table where particle-hole<sup>8,9</sup> or simple shell-model wave functions<sup>5,7</sup> could be assumed for the description of the nuclear states. One purpose of the present work was to determine whether large-basis shell-model wave functions could account for the results of  $(p,p')$  measurements on nuclei with several valence nucleons. A second purpose was the extraction of polarization charges for the valence

protons which could account for core-polarization effects. Using a model for calculating inelastic scattering enhancement factors developed by Atkinson and Madsen<sup>4</sup> and discussed by McManus,<sup>10</sup> we determined polarization charges appropriate to large-basis shell-model calculations in this mass region. Finally, we considered the information on the structure of the shell-model transition densities. A preliminary report of this work has been published elsewhere.<sup>11</sup>

## II. SHELL-MODEL WAVE FUNCTIONS

The shell-model basis space for the wave functions used in the present study consisted of the  $1g_{7/2}$  and  $2d_{5/2}$  orbits, plus one-proton excitations from this subspace into the  $3s_{1/2}$  or  $2d_{3/2}$  orbits. The two-body interaction between the valence nucleons was parameterized in terms of a modified surface-delta-interaction (MSDI), with the four single-particle energies and the two MSDI parameters fixed by making a least-squares fit of model eigenvalues to experimental energies of levels of known  $J^\pi$  in N=82 nuclei.

Two Hamiltonians were investigated. The MSDI parameters for the first<sup>12</sup> were obtained by fitting to levels of known  $J^\pi$  from  $^{136}\text{Xe}$  through  $^{145}\text{Eu}$  (A=136-145), and those for the second<sup>13</sup> by fitting to levels from  $^{136}\text{Xe}$  through  $^{140}\text{Ce}$  (A=136-140). The "A=136-145" interaction was used to calculate wave functions for both  $^{138}\text{Ba}$  and  $^{144}\text{Sm}$ , while the "A=136-140" interaction was designed for the lower mass N=82 isotones, and hence was used only for  $^{138}\text{Ba}$ . Table I lists the single particle energies and

MSDI parameters for both Hamiltonians. The basic difference between them is the  $1g_{7/2}-2d_{5/2}$  single-particle-energy splitting, which was about 500 keV for the A=136-145 interaction and about 900 keV for the A=136-140 interaction.

The results of these shell-model calculations are in generally good agreement with experimental energy-level spectra,<sup>12,13</sup> single-nucleon spectroscopic factors,<sup>14</sup> and relative electro-magnetic transition probabilities,<sup>15</sup> even for nuclides with A<136 whose properties were not included in the search procedure. For  $^{138}\text{Ba}$ , the "A=136-140" theoretical spectrum is in very good agreement with experiment. (See Fig. 1) All theoretical positive parity states for  $E_x < 2.9$  MeV have certain or plausible counterparts in the experimental spectrum, with the single exception of a  $0^+$  state predicted to lie at 2.22 MeV, and the mean deviation of experiment from theory is  $\sim 60$  keV. The "A=136-145" theoretical spectrum for  $^{138}\text{Ba}$  is in slightly less good agreement with experiment. A similar conclusion holds for the other A=134-140, N=82 nuclei and for other observables. This slight preference for the "A=136-140" interaction in the lower N=82 nuclei can be understood as follows. For the upper N=82 isotones, the effects of the limited basis space must be quite important. For example,  $^{144}\text{Sm}$  which has 12 valence protons, effectively has a basis space consisting only of states of the type  $(g_{7/2}-d_{5/2})^{-2}$  and  $(g_{7/2}-d_{5/2})^{-3}(s_{1/2}-d_{3/2})^{+1}$ . The physical low-lying states of  $^{144}\text{Sm}$  presumably have substantial amplitudes in their wave functions for excitations outside of this space, such as  $(1h_{11/2})^2$ ,  $(2d_{3/2})^2$ , and  $(3s_{1/2})^2$ . Including such states in the searching

procedure which determines the parameters of the "A=136-145" Hamiltonian could well distort the parameters to compensate for components outside of the basis space. This would in turn decrease the accuracy of the calculations in the lower isotones. In light of this, the superiority of results calculated for  $^{138}\text{Ba}$  with the "A=136-140" interaction over those calculated with the "A=136-145" interaction is reasonable. Moreover, it is expected that the best results calculated for  $^{138}\text{Ba}$  should be superior to the best for  $^{144}\text{Sm}$ , since the basis space is physically more realistic for A=138. And, indeed, the agreement with experiment for the theoretical results for  $^{144}\text{Sm}$  is substantially inferior to that for  $^{138}\text{Ba}$ . (See Ref. 1)

We have used both the "A=136-140" and "A=136-145" sets of wave functions in the DWBA calculations for  $^{138}\text{Ba}$ , to see if inelastic proton scattering can distinguish between them. Only the "A=136-145" interaction was used in the  $^{144}\text{Sm}$  calculation. With the basis space used in this calculation, states in  $^{138}\text{Ba}$  have between 50 and 220 components in their wave functions, while states in  $^{144}\text{Sm}$  have between 10 and 45 components. In the following discussion we use the notation  $J_i^{\pi}$ , where i refers to the first or second excited state of spin and parity  $J^{\pi}$ .

### III. DWBA ANALYSIS

The microscopic DWBA calculations were performed with the code DWBA70 of Raynal and Schaeffer.<sup>16</sup> The knock-on exchange term, which describes the exchange of coordinates between the

projectile and the valence nucleons of the target, is included in the scattering amplitude. This code is based on the helicity formalism of Raynal<sup>17</sup> which automatically accounts for all values of orbital angular momentum l and spin angular momentum S that can be transferred for a given total angular momentum-parity transfer  $J^{\pi}$ . Central, tensor, and spin-orbit interactions can be included in the two-body force between the projectile and the target nucleons.

It might be noted that, unlike the case for the direct term in the DWBA amplitude, the selection rule  $\Delta r = (-)^l$  does not hold for the exchange term. Thus, four amplitudes characterized by the triads, (LSJ)=(J0J), (J1J), (J-1 1J), and (J+1 1J), can contribute to the cross section, while in the direct term, only the first pair or the second pair can contribute, depending on the parity change. The terms to which the second pair of triads give rise are commonly referred to as non-normal parity amplitudes and are usually small except possibly in the case of transitions to high spin states.<sup>5</sup>

The transition from an initial state with angular momentum and isospin  $J_i, T_i$  to a final state of  $J_f, T_f$  is accomplished by destroying a particle in orbital ( $n'l_i j_i'$ ) and creating a particle in orbital ( $n'l_f j_f'$ ). The transition amplitude is then a sum over contributions from various p-h pairs, each term in the sum being weighted by the spectroscopic amplitude

$$Z_{J_i^{\pi} (j_i')}^{J_f^{\pi} (j_f')} = \frac{\langle T_i T_{m_i} m_i | T_f^{\pi} m_f \rangle}{\langle J_i T_i | | (A_j \times B_{j_i'})^{J_f^{\pi}} | | J_i T_i \rangle} \quad (1)$$



where

$$A_m^j = a_{j,m}^+ \quad (2)$$

$$B_m^j = (-)^{j+m} A_{j,-m} \quad (3)$$

These spectroscopic amplitudes are related to the single particle matrix elements of the spin-angle tensor  $T_{LSJ}$  according to

$$M_{LSJ}^T(jj') = 2\hat{T} \hat{J} \hat{j} \hat{j}' \langle \frac{1}{2} \tau_a, \tau_b - \tau_a | \frac{1}{2} \tau_b \rangle Z(jj') \langle \ell j j' | T_{LSJ}(\theta, \phi, \sigma) | \ell' j' \rangle \quad (4)$$

The quantity  $M_{LSJ}^T(jj')$  is similar to that used by Satchler<sup>5,7</sup> except that it includes isospin quantities.  $\tau_a$  and  $\tau_b$  are the isospin projections of the incident and outgoing projectiles, and  $\hat{X} \equiv \sqrt{2X+1}$ . The procedures used to calculate these  $Z$ 's depend upon the model used to describe the states of the target nucleus. In this work the target states are described by the large-basis shell-model wave functions described in Sec. II. We have modified the Oak Ridge-Rochester shell model codes<sup>18</sup> to calculate the spectroscopic amplitudes  $Z(j j')$  in a form convenient for DWBA calculations.

The transition density is defined in terms of the single-particle matrix elements by

$$F(r) = \sum_{jj'} M_{LSJ}^T(j j') u_{n\ell j}(r) u_{n\ell' j'}(r) \quad (5)$$

where the  $u_{n\ell j}(r)$  are the bound-state radial wave functions for the active valence particles.

In this work we use harmonic oscillator wave functions, which are independent of  $j$ , so the single particle wave functions of interest are  $u_{n\ell} = u_{14}$ ,  $u_{22}$  and  $u_{30}$ , which have 1, 2 and 3 nodes respectively. The transition density will be constructed from a sum

of products of single particle wave functions, each product being weighted by the appropriate  $M_{LSJ}^T(jj')$ . It is clear that a term such as  $u_{14} u_{14}$  will contribute a simple shape with a single maximum, while a term such as  $u_{22} u_{30}$  has several maxima and minima. The magnitude of each  $M_{LSJ}^T(jj')$  is related to the coherence properties of the amplitudes of the components of the wave functions; in general a larger  $M_{LSJ}^T(jj')$ , results from constructive interference between the amplitudes while a small number results from destructive interference. Hence, there are two aspects of the transition density which affect the cross section-- the first being the magnitude of the individual components  $M_{LSJ}^T(jj')$ , and the second being the interference among the terms of the sum in Eq. 5. Different shell model wave functions will give different  $Z^{JT}(jj')$ , thus different  $M_{LSJ}^T(jj')$ , and hence transition densities of different shape.

The form factor,  $G_{(r)}^{LSJ,T}$ , for the direct term of the scattering amplitude is related to the transition density through the relation

$$G_{(r)}^{LSJ,T} = \int F(r') \{ V_L^{ST}(r,r') r' \}^2 dr' \quad (6)$$

where  $V_L^{ST}(r,r')$  is the  $L^{\text{th}}$  multipole in the decomposition of the two-body force between the bound nucleon and the incident projectile. The form factor  $G_{(r)}^{LSJ,T}$  thus contains all of the nuclear structure information put into the analysis in addition to the assumptions made for the interaction between the projectile and target nucleons.

Finally, the form factor is folded in with the incident and exit channel optical-model wave functions and squared to get the direct contribution to the DWBA cross section.

The previous discussion has been concerned only with the direct DWBA contribution to the scattering amplitude. The transition density is not defined as such for the exchange amplitude, since for exchange, the initial and final bound state wave functions have different radial co-ordinates. However, a quantity corresponding to  $M_{LSJ}^T(jj')$  for the direct term exists for the exchange term,<sup>5</sup> and can be used to obtain an estimate of the magnitude of the exchange contribution to a given transition. In the case of the exchange amplitude, the form factor is different for each pair of partial waves, and involves many multipoles of the two-body force for a given orbital angular momentum transfer  $L$ .

The pertinent details of the inelastic scattering calculation are as follows. The optical model parameters labeled Set SII and Set SI in Ref. 1 are used to describe the incident and exit channels of  $^{138}\text{Ba}$  and  $^{144}\text{Sm}$ , respectively. The bound states are described by harmonic oscillator wave functions. The harmonic oscillator constant for the bound state wave functions is obtained from

$$k_w = \frac{45}{A^{1/3}} - \frac{25}{A^{1/3}} \quad (7)$$

The two-body interaction between the projectile and target nucleons is assumed to contain only central terms with a Serber exchange mixture and a Yukawa radial dependence.

Thus

$$V_{ip}(r) = [V_{00} + V_{10} \bar{\sigma}_i \cdot \bar{\sigma}_p + V_{01} \bar{\tau}_i \cdot \bar{\tau}_p + V_{11} (\bar{\sigma}_i \cdot \bar{\sigma}_p) (\bar{\tau}_i \cdot \bar{\tau}_p)] \frac{e^{-r/\mu}}{r/\mu} \quad (8)$$

where  $\mu$  is the range of the force,  $i, p$  label the valence nucleons and the projectile, respectively and the subscripts on the  $V_{ST}$  are the spin and isospin transferred in the reaction. For a Serber interaction  $V_{00}:V_{10}:V_{01}:V_{11} = -3:1:1:1$ .

The strength of the largest of the  $V_{ST}$  was taken as the mean value found in the tabulation of Austin,<sup>2</sup>  $V_{00} = -27.8$  MeV for a range  $\mu = 1.0$  F. It was found in preliminary calculations that  $\mu = 1.4$  F provided a somewhat better fit to the shape of the angular distributions. The value of  $V_{00}$  ( $\mu = 1.4$  F) = -12.6 MeV used in the calculations was fixed so as to give the same cross section in a DWBA calculation for the  $2_1^+$  state in  $^{138}\text{Ba}$  as did the 1.0 F. range force. Since our wave functions contain only proton orbitals, the number which actually enters the calculations is  $V_{pp}^S = V_{SO} + V_{S1}$ , which is -8.4 MeV for the dominant  $S=0$  part of the proton-proton interaction. Coulomb excitation was not included in the calculations.

#### IV CORE POLARIZATION

The effects of core polarization, i.e., effects from nucleons outside the explicit shell-model basis space, must be included for an account of the absolute magnitudes of inelastic scattering<sup>19</sup> in any calculation of the type considered here. In the case of electromagnetic transitions these effects are also manifest and are accounted for by renormalizing the charge on the nucleons, i.e., by introducing a "polarization charge". Madsen<sup>4,10</sup> has shown that one can similarly correct for finite basis-space effects in



inelastic scattering by renormalizing the strength of the two-body force which mediates the transition. Thus one has an "effective force" for  $(p,p')$  which is analogous to the "effective charge" for electromagnetic transitions. The major assumption involved in obtaining this result is that the ratios of the inelastic scattering single particle amplitudes (direct plus exchange) to the corresponding electromagnetic amplitudes are independent of the single-particle quantum numbers. This is rigorously true for the direct amplitude in the plane-wave Born approximation at zero momentum transfer. Atkinson and Madsen<sup>4</sup> have shown by numerical calculation that this assumption is good to within approximately 10% for a specific DWBA example.

One can estimate the enhancement factor directly from Madsen's formulation. However, we proceed in a more heuristic fashion. To estimate the core contributions to transition strengths for the low-lying states of  $^{138}\text{Ba}$ , we note that for the wave functions used here, the calculated  $B(E2; 2^+_1, 0^+_1)$  is a factor of 3.2 too small<sup>15</sup> if no polarization charge  $\delta e$  is used. This implies that the effective proton charge,  $(1+\delta e)^2=3.2$ , or the polarization charge,  $\delta e=0.8$ , in electron charge units. To account for the contribution to the  $(p,p')$  reaction of protons excited from the core, one therefore renormalizes the interaction strength  $V_{pp}$  to  $(1+\delta e)V_{pp}$ . However, excitations of neutrons from the core also contribute to the  $(p,p')$  cross sections and, in fact, are more important than those of protons, since the proton-neutron two-body interaction,  $V_{pn}$ , is stronger than  $V_{pp}$ .

If it is assumed, as has been suggested by Bernstein<sup>20</sup> and Astner, et al.,<sup>21</sup> that contributions from neutron and proton core excitations are approximately in the ratio of  $N/Z$  (the ratio expected in a collective model picture), we need an additional term,  $N/Z \delta e V_{pn}$  in the effective interaction to account for neutron core excitations. For the Serber exchange mixture we have used,  $V_{pn}=2V_{pp}$ . Thus one obtains a total effective force of  $(1+\delta e)V_{pp} + 2(N/Z)\delta e V_{pp} = [1+\delta e(1+2N/Z)]V_{pp}$ , i.e. the strength is increased by a factor of  $(1+\delta e(1+2N/Z))$ . This corresponds to a cross section enhancement of 17.2 for  $\delta e=0.8$ .

We have used this factor of 17.2 to normalize the DWBA results for all states in both  $^{138}\text{Ba}$  and in  $^{144}\text{Sm}$ , as these predictions are shown in Figures 2-4. That is, the figures show essentially a priori  $(p,p')$  calculations based upon an assumed polarization charge of 0.8e (i.e., a total proton charge of 1.8e).

It is clear from Figs. 2 and 3 that while  $\delta e=0.8$  is a reasonable estimate for all states, fluctuations do occur. To determine best values of  $\delta e$  for individual states we start with the ratio of the "bare" DWBA predictions to the experimental data. If an enhancement factor is defined as  $\epsilon = \frac{\sigma}{\sigma_{\text{theory}}}$  for a state, then, following the assumptions and choices just outlined, the corresponding polarization charge is obtained from

$$[1+\delta e(1+\frac{2N}{Z})]^2 = \epsilon. \quad (9)$$

We have determined the polarization charges so defined for each of the states of  $^{138}\text{Ba}$  under study. The results are presented

in Table II. The enhancement factors used were extracted from the ratios of the experimental and theoretical cross sections each integrated over the angular range of the measurements.

To estimate the accuracy of the numbers thus obtained, we consider the effects of uncertainties in the input numbers. First,  $V_{00}$  is perhaps known to within  $\pm 15\%$ , which corresponds to an uncertainty of  $\pm 0.16$  in  $\delta\epsilon$ . Uncertainties introduced by possible variations from a Serber force are not large (about  $\pm 0.04$  in  $\delta\epsilon$ ) because, for example, an increase in  $V_{01}$  leads to a decrease in  $V_{pp}$  but an increase in  $V_{pn}/V_{pp}$ , and these effects almost cancel. If we assign to the ratio of neutron and proton polarization charges a fifty percent uncertainty, the corresponding uncertainty in  $\delta\epsilon$  is  $\pm 0.10$ . The usual DWBA uncertainties for inelastic scattering are perhaps  $\pm 20\%$  in cross section corresponding to an uncertainty in  $\delta\epsilon$  of  $\pm 0.11$ . Finally the uncertainty of  $\pm 10\%$  in the experimental normalization contributes an uncertainty of  $\pm 0.05$ . Adding these in quadrature one obtains an uncertainty of  $\delta\epsilon = \pm 0.23$ . Most of these effects change the numbers for different  $L$  transfers in the same way so the relative values of  $\delta\epsilon$  are perhaps better known than this. On the other hand, we have neglected the basic uncertainty in the approximation that the ratios of the corresponding scattering and electromagnetic amplitudes are independent of the single particle quantum numbers. If Madsen's estimate were valid here, our  $\delta\epsilon$  would be large by 0.1 for the  $2^+$  states. It is possible the overestimate is larger for the higher spin states, where exchange effects are more important.

## V. RESULTS

For  $^{138}\text{Ba}$ , we have calculated angular distributions using both sets of wave functions ("A=136-140" and "A=136-145" Hamiltonians) for the aforementioned  $2^+$ ,  $4^+$ , and  $6^+$  states. Figures 2 and 3 show the angular distributions predicted by each set of wave functions, together with the appropriate data from Ref. 1. All theoretical cross sections include the enhancement factor of 17.2. The knock-on exchange amplitude contributes substantially to all cross sections and especially to those for the high spin states. We see that the magnitudes and shapes of the calculated angular distributions are in good agreement with the data for the  $2_1^+$ ,  $4_1^+$ , and  $6_1^+$  states for both sets of wave functions, except that the first maximum of the  $2^+$  is predicted too far forward.

The agreement between theory and experiment for the  $2_2^+$ ,  $4_2^+$ , and  $6_2^+$  states, however, is much better for the "A=136-140" set of wave functions than for the "A=136-145" set. The latter yield cross sections which are an order of magnitude low and which also do not fit the experimental shapes well. This comparison indicates that the "A=136-140" wave functions give the better description of the low-lying states of  $^{138}\text{Ba}$ . The most salient point, we think, is that the single multiplicative enhancement factor suffices to produce essentially the right magnitudes for all six states. Hence, it is suggested that with good wave functions and with DWBA including exchange, a state independent effective force is appropriate.



Only the "A=136-145" Hamiltonian was applicable to  $^{144}\text{Sm}$ , so only the set of wave functions corresponding to this interaction was employed in the DWBA calculations. For comparison purposes we have used the same enhancement factor (17.2) as for  $^{138}\text{Ba}$ , a value which is reasonably consistent with the polarization charge of  $1.02 \cdot 0.17$  obtained from the measured  $2^+ \rightarrow 0^+$  B(E2) value<sup>22</sup> in  $^{144}\text{Sm}$  and the B(E2) calculated from the "A=136-145" wave functions.<sup>15</sup> The results are shown in Fig. 4. The angular distribution for the  $4^+_1$  state is a factor of two smaller than the data at forward angles, but the inadequacy of the model for  $^{144}\text{Sm}$  is most apparent when one considers the calculation for the  $2^+_2$  state. All of the strength has been concentrated in the  $2^+_1$  state, the angular distribution for the  $2^+_2$  state falling a factor of 25 below the data. In addition, the shape is not qualitatively correct; the maximum at  $40^\circ$  is larger than that at  $20^\circ$ . The calculated  $4^+_2$  angular distribution is a factor of 3 lower than the data, while the calculation for the  $6^+_2$  bears no resemblance to the data. As is obvious from Fig. 4 a constant polarization charge does not reproduce the magnitude of the angular distribution for different L-transfers. Here, in contrast to  $^{138}\text{Ba}$ , a state dependent polarization charge is required.

We have performed calculations including tensor forces corresponding to the one-pion-exchange potential,<sup>2</sup> and find that the tensor force contributions to the cross section are at most 7%. This occurs for the  $6^+$  states, for which the non-normal exchange amplitudes are non-negligible.<sup>5</sup> The spin-orbit force may also be important<sup>24</sup> for the  $6^+$  states; this possibility is being investigated further.

Finally, we have calculated cross sections for transitions to the non-normal parity  $3^+$  and  $(5^+)$  states at 2.445 and 2.415 MeV, respectively. These cross sections are not expected to be strongly affected by collective effects, but may be sensitive to tensor and spin-orbit terms in the effective interaction. The tensor force used corresponded<sup>2</sup> to the one-pion-exchange potential while the spin-orbit force was obtained from the Hamada-Johnston potential<sup>25</sup> with a cutoff radius of 0.6 F as described in Ref. 2. This force is somewhat weaker than that used by Love.<sup>24</sup> As is seen in Fig. 5, the tensor and spin-orbit forces are indeed important, but the theoretical cross section is a factor of 3-5 below the data. More complex reaction mechanisms such as those involving multistep processes may be important for these weakly excited states.

## VI. DISCUSSION

To understand the roots of the different results for  $^{138}\text{Ba}$  obtained with the two different sets of wave functions, recall that all of the nuclear structure information entering the DWBA calculation is contained in the transition densities such as those shown in Figs. 6 and 7. The magnitude of the transition density is plotted versus the radial coordinate expressed in units of  $r_0 A^{1/3}$ ; thus unity corresponds to the nuclear surface. Inspection (Fig. 6) shows that the transition densities for the  $2^+_1$ ,  $4^+_1$ , and  $6^+_1$  states are quite similar for both sets of wave functions. They peak slightly inside the nuclear surface, which is a general characteristic<sup>23</sup> of these quantities. We recall

that the cross sections calculated for these states were very similar for both sets of wave functions. However, there are distinct differences between the transition densities predicted for each of the  $2_2^+$ ,  $4_2^+$ , and  $6_2^+$  transitions. The "A=136-145" wave functions, relative to the "A=136-140" wave functions, yield transition densities with a pronounced decrease in magnitude of the peak near the surface and an increase in the magnitude of the peak near 0.6 of the nuclear radius. For the  $6_2^+$  state, this effect is so great that the transition density resembles that for a much lighter nucleus. Since the transition density (and therefore the form factor) peaks far inside the nuclear surface for this transition, the diffraction pattern predicted by the DWBA should be pushed out, as if the target nucleus were indeed much lighter. This is exactly what we observe for the calculated  $6_2^+$  cross sections for the "A=136-145" set of wave functions in 138Ba and 144Sm.

We can infer specifically what is wrong with this set of wave functions by considering as an example the individual contributions to the total transition density for the  $6_2^+$  state in 138Ba. Figure 7 shows both this transition density and its component parts, which are proportional to  $u_{14}u_{14}$  and  $u_{14}u_{22}$ . For the "A=136-140" set of wave functions the  $u_{14}u_{22}$  term is large relative to the  $u_{14}u_{14}$  term, which results in the surface peaking. However, the components are about the same size for the "A=136-145" wave function, and cancellation makes the transition density very small at the surface. If we now look at the spectroscopic amplitudes

which contribute to  $u_{14}u_{14}$  and  $u_{14}u_{22}$  we can study the wave functions directly. Only the  $M_{TSJ}^T(j j') = M_{606}^0(g_{7/2}, g_{7/2})$  matrix element contributes to  $u_{14}u_{14}$ , while both  $M_{606}^0(g_{7/2}, d_{5/2})$  and  $M_{606}^0(d_{5/2}, g_{7/2})$  contribute to the  $u_{14}u_{22}$  term of the sum. Table III shows the structure of the largest components of the pertinent wave functions, as well as the individual contributions to the  $6_2^+$  transition density calculated with both sets of wave functions. The two transition densities are thus

$$F_{606,0} = 0.1292 u_{14}u_{14} + 0.3223 u_{14}u_{22} \quad \text{"A=136-140"}$$

$$F_{606,0} = 0.1765 u_{14}u_{14} + 0.1978 u_{14}u_{22} \quad \text{"A=136-145"}$$

The quantity of interest is the ratio  $u_{14}u_{22}/u_{14}u_{14}$  which has the values 2.50 and 1.12 for the "A=136-140" and "A=136-145" interactions, respectively. The major reason for the smaller ratio from the "A=136-145" wave function is the small size of the  $u_{14}u_{22}$  contribution. This set of wave functions has the smaller  $g_{7/2}-d_{5/2}$  single particle splitting and might naively be expected to have the larger  $u_{14}u_{22}$  term; a detailed comparison of the wave functions in Table III shows why this is not so. The largest contributions to  $u_{14}u_{22}$  for the "A=136-140" set come from the  $(g_7)^6 (g_7)^5 (d_5)^1$  and  $(g_7)^4 (d_5)^2 + (g_7)^4 (d_5)^2$  amplitudes, which for the "A=136-145 wave" functions are much smaller, because the smaller  $g_{7/2}-d_{5/2}$  splitting leads to a fragmentation of the strength of the  $6_2^+$  wave functions over many components. Many of these components cannot be connected by the one body (p,p') operator to the strong components of the much less fragmented ground state, and hence do not contribute significantly



to the transition density. It thus appears that decreased mixing between the  $g_{7/2}$  and  $d_{5/2}$  orbitals is the required ingredient in obtaining a reasonable fit to the angular distribution for the  $6_2^+$  state. A similar analysis applied to the transition densities for the  $4_2^+$  states arrives at the same conclusion--namely that there appears to be too much mixing of the  $g_{7/2}$ - $d_{5/2}$  orbitals in the higher lying states as calculated with the "A=136-145" interaction. Specific information about the structure of the wave functions can thus be inferred by analyzing the composition of the transition densities in this manner.

The previous discussion has been concerned only with the direct DWBA contribution to the scattering amplitude. However, it has been found<sup>4,26</sup> that the direct and exchange amplitudes are constructively coherent in general, and identically so for a zero-range, even-state force. Atkinson and Madsen<sup>4</sup> have done a particularly complete study of the properties of the direct and exchange amplitudes for transitions in single-closed-shell nuclei (such as the N=82 nuclei), including the same single particle orbitals arising in the present work. They find that, with a Serber force, the shapes of the exchange contributions to the angular distributions are very similar to those for the direct term. Since we have also used a Serber force, the previous transition density discussion hopefully remains valid when the exchange amplitude is included, the main effect of the exchange amplitude being a renormalization of the magnitude of the cross section.

Comparing the DWBA calculations resulting from the collective model (Ref. 1) and microscopic model (Fig. 2) for the  $2_1^+$  state, we see that the collective model does a somewhat better job of fitting the data. We have performed a collective model calculation with the form factor obtained by deforming only the real part of the optical model potential, and obtained an angular distribution nearly identical to the angular distribution predicted by microscopic model. We conclude that if one were to combine the form factor obtained by deforming the imaginary part of the optical model with the real form factor used in the microscopic analysis, the resulting angular distribution would be in as good agreement with the data as that of the full deformed collective model. Indeed, it has recently been found that using a complex microscopic form factor results in appreciably better fits to angular distribution<sup>27</sup> and asymmetry<sup>28</sup> data in other nuclei. It would also be interesting to determine whether the addition of an imaginary term to the form factor, which presumably would improve the fit to the  $2_1^+$ , would destroy the relatively good fits to the  $4_1^+$  and  $6_1^+$  states obtained with the present microscopic approach and whether its inclusion would require a state dependent polarization charge. Such calculations are presently underway.

It should be noted that our calculations use a multiplicative constant in the form factor to account for core polarization and hence that the angular distributions have the shape predicted

by the purely microscopic calculation. Other microscopic calculations<sup>19</sup> have frequently employed an additive term, based on the collective model, in the form factor to simulate the effects of core polarization. Often in this latter procedure the collective term dominates the cross section, so that the predicted shape for the angular distribution is in reality that of the collective-model contribution. Thus, such "microscopic" calculations yield good fits to experimental shapes because collective model predictions are usually better in this regard than those of a purely microscopic model such as that we have used.

The above considerations seem to support the use of an additive collective model form factor to account for core polarization effects. However, the effective-charge approach used here has the important advantage of reflecting the apparent fact that the participation of the core is approximately proportional to the transition strength due to the valence orbitals alone. In the case of the  $2^+$  state in  $^{138}\text{Ba}$  for example, the cross section (and hence in major part the core contribution) for the  $2_1^+$  state is about four times that for the  $2_2^+$  state. Yet both are given correctly by the same multiplicative renormalization.

#### VII. SUMMARY

Microscopic DWBA calculations including the exchange amplitude were performed for the  $2_1^+$ ,  $4_1^+$ ,  $2_2^+$ , and  $6_1^+$  states in  $^{138}\text{Ba}$  and  $^{144}\text{Sm}$ , using shell model wave functions,<sup>12,13</sup> a realistic two-nucleon

force, and an enhancement factor calculated using the effective charge model of Madsen.<sup>4</sup> The necessary structure amplitudes were calculated with a modified version of the Oak Ridge-Rochester shell model code. In the case of  $^{138}\text{Ba}$ , calculations were made with two sets of shell model wave functions and it was determined that inelastic proton scattering cross sections clearly distinguished one set as quite satisfactory and superior to the other. The transition densities, which provide the link between the wave functions and the DWBA reaction model, were analyzed to determine the undesirable properties of the poorer set of wave functions. It was found that the large mixing between the  $g_{7/2}$  and  $d_{5/2}$  orbitals in the "A=136-145" wave functions led to the poorer result. We find that a careful consideration of the transition density between two states can provide useful information concerning the structure of the wave functions for these states. Predictions of the cross sections for  $^{144}\text{Sm}$  were much less satisfactory than those for  $^{138}\text{Ba}$ , presumably because the shell-model basis employed is unphysically restricted for  $^{144}\text{Sm}$ . The contributions of core excitations to the cross section were stronger by about a factor of 20 than those of the valence protons for the low-lying  $2^+$ ,  $4^+$ , and  $6^+$  states of  $^{138}\text{Ba}$  and  $^{144}\text{Sm}$ . However, in the case of  $^{138}\text{Ba}$  it was found that a state and multipole independent effective charge described the core polarization contributions to the cross sections within about 25%. This implies that the core participation for a given state in  $^{138}\text{Ba}$  is approximately proportional to the transition strength due to the valence orbitals.



It is perhaps worth pointing out here that inelastic proton scattering is extremely sensitive to neutron configurations because the proton-neutron force is approximately twice the proton-proton force. This sensitivity is what leads to an enhancement factor of 17.2 in the  $(p,p')$  cross section, over five times larger than the corresponding enhancement of electromagnetic transitions (3.2). It also makes  $(p,p')$  studies a valuable complement to inelastic electron scattering, which is mostly sensitive to proton configurations, in studies of the isospin structure of core excitations.

Finally we note that the program developed in this work for the calculation of the spectroscopic amplitudes was a modification of the Oak Ridge-Rochester shell model codes<sup>18</sup> and can be used whenever wave functions obtained with this code are available. Such wave functions now exist for most nuclei up through the nickel isotopes, and for the zirconium, N=82, and lead regions, making it straight forward to treat inelastic scattering in a consistent microscopic fashion over a large part of the nuclidic chart.

#### ACKNOWLEDGEMENTS

We wish to thank H. McManus and F. Petrovich for enlightening conversations and assistance, and R. Schaeffer for making the code DWBA70 available. We are also grateful to J. McGroory for assistance with the Oak Ridge-Rochester shell model codes.

#### REFERENCES

1. D. Larson, S. M. Austin and B. H. Wildenthal, *Phys. Rev. C* **9**, 1574(1974).
2. S. M. Austin in The Two-Body Force in Nuclei, eds. S. M. Austin and G. M. Crawley (Plenum Press, New York, 1972).
3. F. Petrovich, H. McManus, V. Madsen and J. Atkinson, *Phys. Rev. Letts.* **22**, 895(1969); F. Petrovich, H. McManus, J. Borysowicz and G. R. Hammerstein, to be published; J. Borysowicz, H. McManus and G. Bertsch, to be published.
4. J. Atkinson and V. A. Madsen, *Phys. Rev. C* **1**, 1377(1970).
5. W. G. Love and G. R. Satchler, *Nucl. Phys.* **A159**, 1(1970).
6. G. R. Satchler, *Particles and Nuclei* **5**, 77(1973).
7. G. R. Satchler, *Nucl. Phys.* **77**, 481(1966).
8. S. M. Austin, P. J. Locard, S. N. Bunker, J. M. Cameron, J. R. Richardson, J. W. Verba and W.T.H. vanOers, *Phys. Rev.* **C3**, 1514(1971).
9. R. Reif and J. Höhn, *Nucl. Phys.* **A137**, 65(1969).
10. H. McManus, in The Two-Body Force in Nuclei, eds. S. M. Austin and G. M. Crawley (Plenum Press, New York, 1972).
11. D. Larson, S. M. Austin, and B. H. Wildenthal, *Phys. Letters* **42B**, 153(1972).
12. B. H. Wildenthal, *Phys. Rev. Letters* **22**, 1118(1969).
13. B. H. Wildenthal and D. Larson, *Phys. Letters* **37B**, 266(1971).
14. B. H. Wildenthal, *Phys. Letters* **29B**, 274(1969).
15. D. Larson and B. H. Wildenthal, *B.A.P.S.* **17**, 512(1972).
16. R. Schaeffer and J. Raynal, unpublished.
17. J. Raynal, *Nucl. Phys.* **A97**, 572(1967).

18. J. B. French, E. C. Halbert, J. B. McGrovy and S.S.M. Wong, in Advances in Nuclear Physics, Vol. III, eds. M. Baranger and E. Vogt (Plenum Press, New York, 1969).
19. W. G. Love and G. R. Satchler, Nucl. Phys. A101, 424(1967).
20. A. M. Bernstein, Phys. Letters 29B, 335(1969).
21. G. Astner, I. Bergström, J. Blomqvist, B. Fant, and K. Wikström, Nucl. Phys. A182, 219(1972).
22. D. Eccleshall, M.J.L. Yates, and J. J. Simpson, Nucl. Phys. 78, 481(1966).
23. F. Petrovich, Michigan State University Thesis, 1970 (unpublished).
24. W. G. Love, Phys. Letters 35B, 371(1971).
25. T. Hamada and I. D. Johnston, Nucl. Phys. 34, 382(1962).
26. J. Atkinson and V. A. Madsen, Phys. Rev. Letters 21, 295(1968).
27. G. R. Satchler, Phys. Letters 35B, 279(1971).
28. R. H. Howell and G. R. Hammerstein, Nucl. Phys. A192, 651(1972).
29. E. C. Halbert, J. B. McGrovy, B. H. Wildenthal, and S. P. Pandya, in Advances in Nuclear Physics, Vol. IV, eds. M. Baranger and E. Vogt (Plenum Press, New York, 1972).

## FIGURE CAPTIONS

Figure 1. Comparison of results of shell model calculations discussed in Sec. II with experimentally known energy levels in  $^{138}\text{Ba}$ .

Figure 2. Microscopic model DWBA calculations for the inelastic scattering to the  $2_1^+$ ,  $4_1^+$ , and  $6_1^+$  states in  $^{138}\text{Ba}$ . The calculations are identical except for the wave functions; the left hand column employed the "A=136-140" set while the "A=136-145" set was used for the right hand column. The cross section enhancement factor was calculated for  $\delta e=0.8$ . The dashed curve is the contribution of the direct amplitude while the solid curve contains the contributions of both the direct and exchange amplitudes.

Figure 3. Microscopic model DWBA calculations for the inelastic scattering to the  $2_2^+$ ,  $4_2^+$ , and  $6_2^+$  states in  $^{138}\text{Ba}$ . The cross section enhancement factor was calculated for  $\delta e=0.8$ . For other details see the caption of Fig. 2.

Figure 4. Microscopic model DWBA calculations for inelastic scattering to the  $2_{1,2}^+$ ,  $4_{1,2}^+$ , and  $6_{1,2}^+$  states in  $^{144}\text{Sm}$  calculated with the "A=136-145" set of wave functions. The cross section enhancement factor was calculated with  $\delta e=0.8$ .

Figure 5. Microscopic model DWBA calculations for inelastic scattering to the  $3_1^+$  and  $(5_1^+)$  states in  $^{138}\text{Ba}$  calculated with the "A=136-140" set of wave functions. The two-body force included central, tensor and L-S terms, but no collective renormalization was included.

Only the (Direct + Exchange) calculations are shown.

Figure 6. Transition densities for the  $2_{1,2}^+$ ,  $4_{1,2}^+$ , and  $6_{1,2}^+$  states in  $^{138}\text{Ba}$  calculated with both sets of wave functions.

Figure 7. Composition of the  $6_2^+$  transition density in  $^{138}\text{Ba}$ , calculated with both sets of wave functions. The left hand figure is calculated with the "A=136-140" set while the right hand figure is calculated with the "A=136-145" set. The unlabeled line is the total transition density, the sum of the other two curves.

Table I. Parameters of the MSDI  $V = -4\pi A \delta(r_i - r_j) f_{ij} + B^a$  and single particle energies used for the calculation of the wave functions.

Parameter	$^A=136-140$ Interaction [MeV]	$^A=136-145$ Interaction [MeV]
A	0.373	0.382
B	0.507	0.517
$E_{g7/2}$	-9.526	-9.451
$E_{d5/2}$	-8.646	-8.970
$E_{d3/2}$	-6.626	-6.334
$E_{s1/2}$	-6.576	-6.438
$E_{g7/2} - E_{d5/2}$	0.880	0.481
$E_{g7/2} - E_{d3/2}$	2.900	3.117
$E_{g7/2} - E_{s1/2}$	2.950	3.013

<sup>a</sup>The notation is that used in Ref. 29.

Table II. Effective charges for transitions in <sup>138</sup>Ba.

Transition	L <sub>p</sub>	δe <sup>c</sup>
0 <sup>+</sup> →2 <sub>1</sub> <sup>+</sup>	2	0.82±0.23
0 <sup>+</sup> →4 <sub>1</sub> <sup>+</sup>	4	0.86±0.23
0 <sup>+</sup> →6 <sub>1</sub> <sup>+</sup>	6	0.61±0.23
0 <sup>+</sup> →2 <sub>2</sub> <sup>+</sup>	2	0.98±0.23
0 <sup>+</sup> →4 <sub>2</sub> <sup>+</sup>	4	1.07±0.23
0 <sup>+</sup> →(6 <sub>2</sub> <sup>+</sup> ) <sup>a</sup>	6	0.73±0.23

<sup>a</sup>This state has not been unambiguously assigned 6<sup>+</sup>, but its angular distribution, together with the shell-model predictions, suggest this assignment.

<sup>b</sup>This is the L-transfer for the dominant amplitude. Non-normal parity amplitudes also contribute to the cross section and are included in the calculations. See Ref. 5.

<sup>c</sup>Calculated using Eq. 9.

<sup>a</sup>The subscripts on the single particle orbitals are 2j i.e. 8<sub>7/2</sub> = 8<sub>7</sub>.

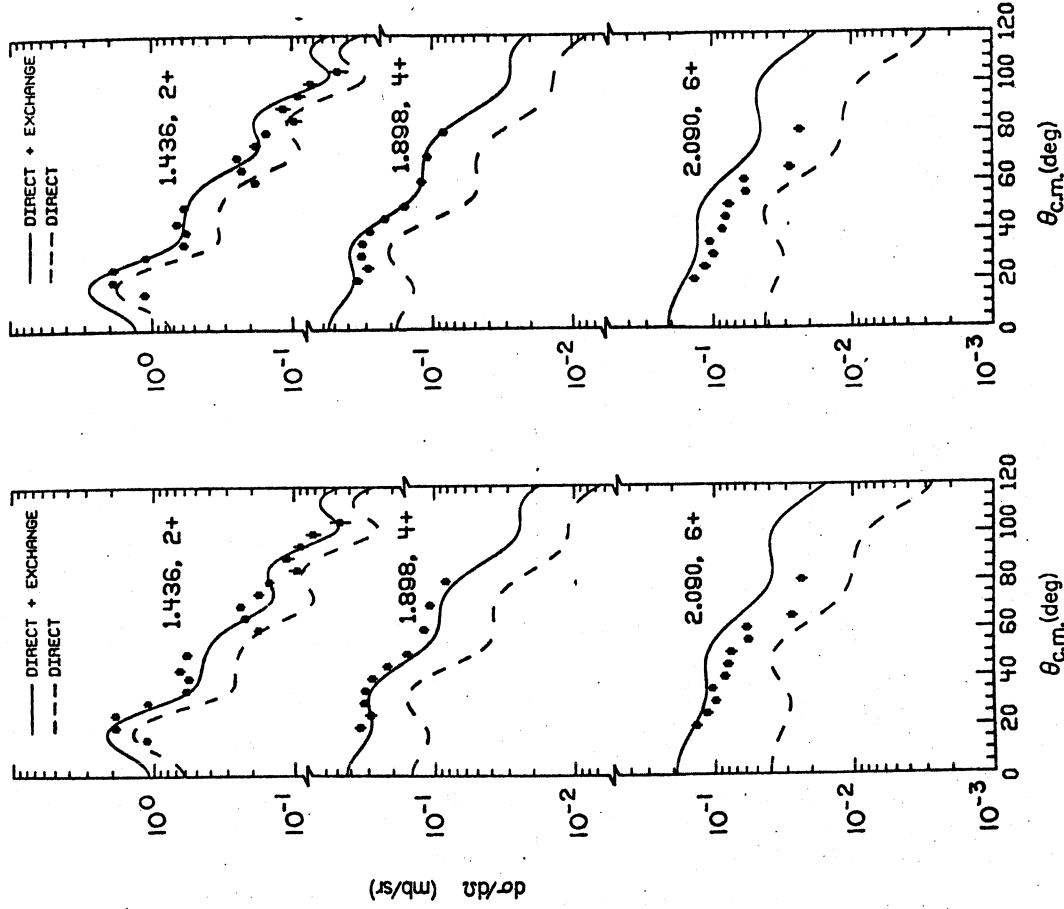
$ 0^+\rangle_{g.s.} = -0.675 (g_7)^6 \rangle - 0.286 (g_7)^4 \rangle$	$ 0^+\rangle_{g.s.} = -0.517 (g_7)^6 \rangle - 0.740 (g_7)^4 \rangle$	$ 0^+\rangle_{g.s.} = 0.599 (g_7)^6 \rangle - 0.559 (g_7)^5 \rangle - 0.318 (g_7)^3 \rangle - 0.316 (g_7)^4 \rangle$	$ 0^+\rangle_{g.s.} = 0.573 (g_7)^6 \rangle - 0.303 (g_7)^5 \rangle - 0.246 (g_7)^3 \rangle - 0.621 (g_7)^4 \rangle$
"A=136-140"	"A=136-145"	"A=136-140"	"A=136-145"
$M_{606}^{606}(g_{7/2}, d_{5/2})$	$M_{606}^{606}(g_{7/2}, g_{7/2})$	$M_{606}^{606}(d_{5/2}, d_{5/2})$	$M_{606}^{606}(d_{5/2}, g_{7/2})$
0.675	0.517	0.599	0.573
0.286	0.740	0.318	0.246
0.2174	0.1292	0.1049	0.0800
0.1178	0.1765	0.2174	0.1178

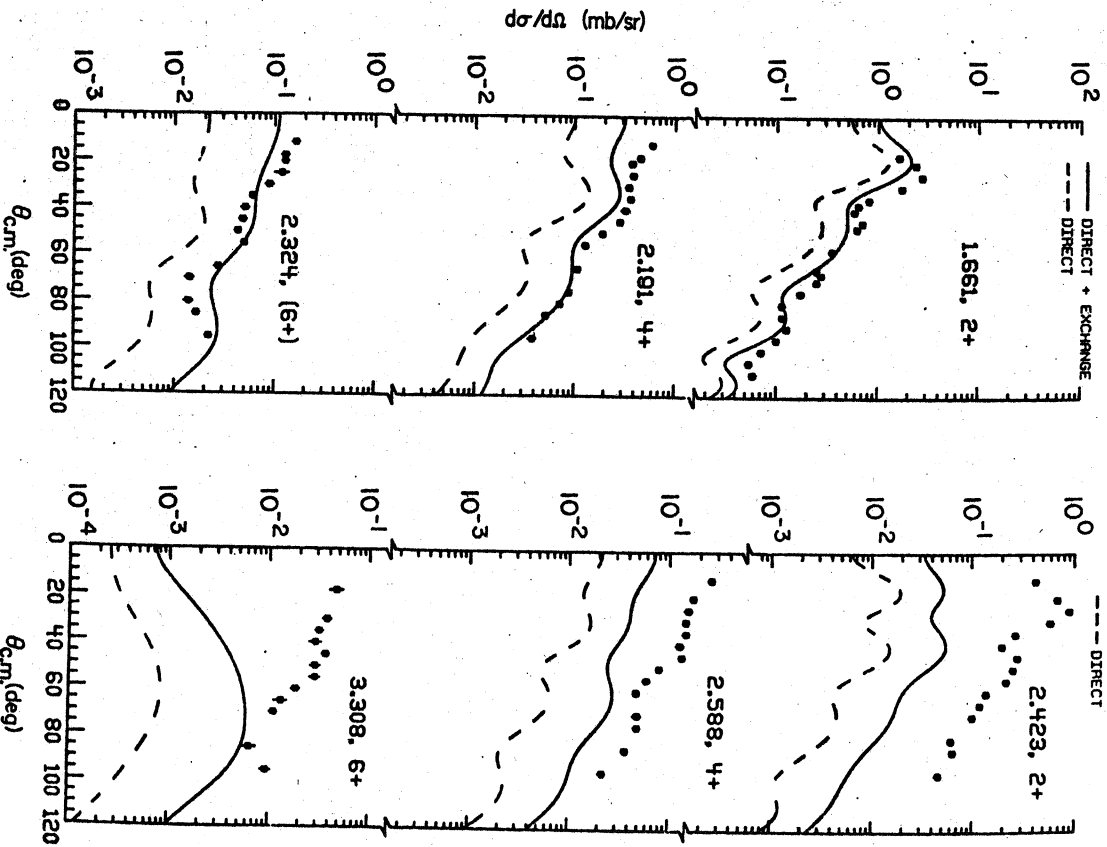
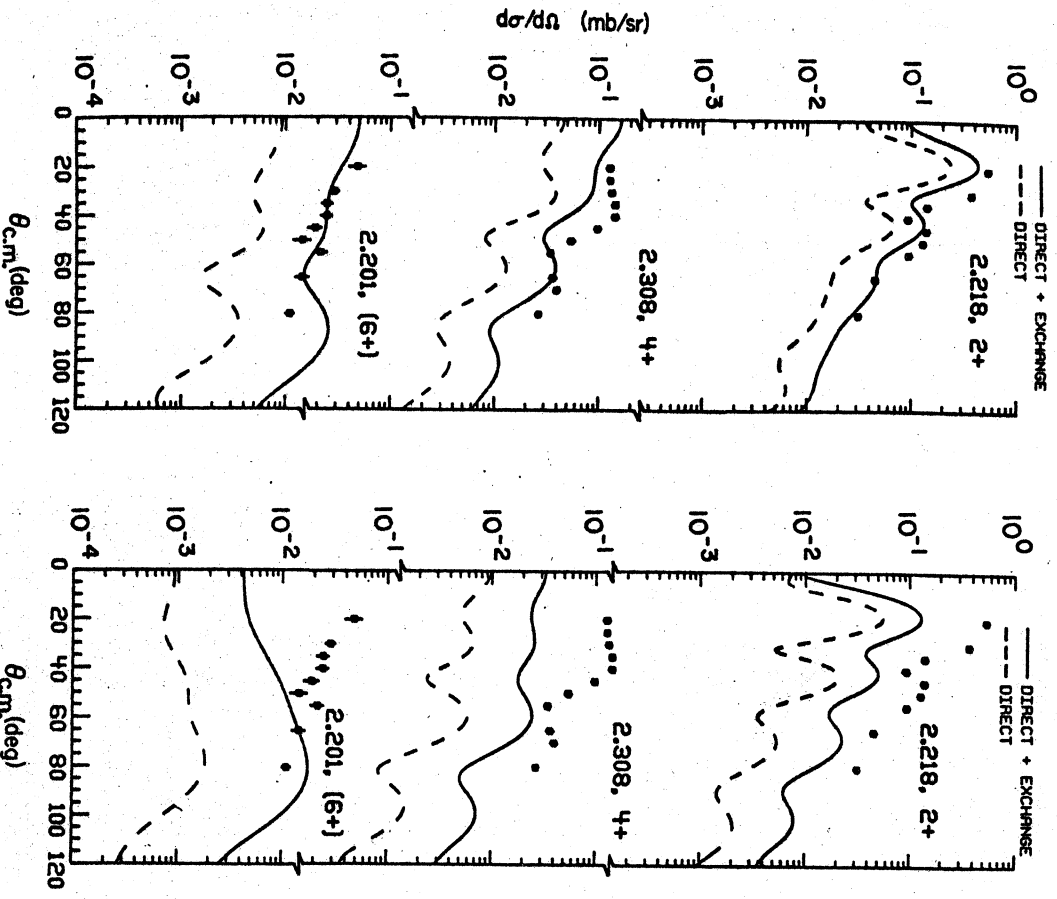
Table III: Major components of 0<sup>+</sup> and 6<sup>+</sup> wave functions<sup>a</sup> calculated with both interactions, and the resulting matrix elements for the associated transition densities.



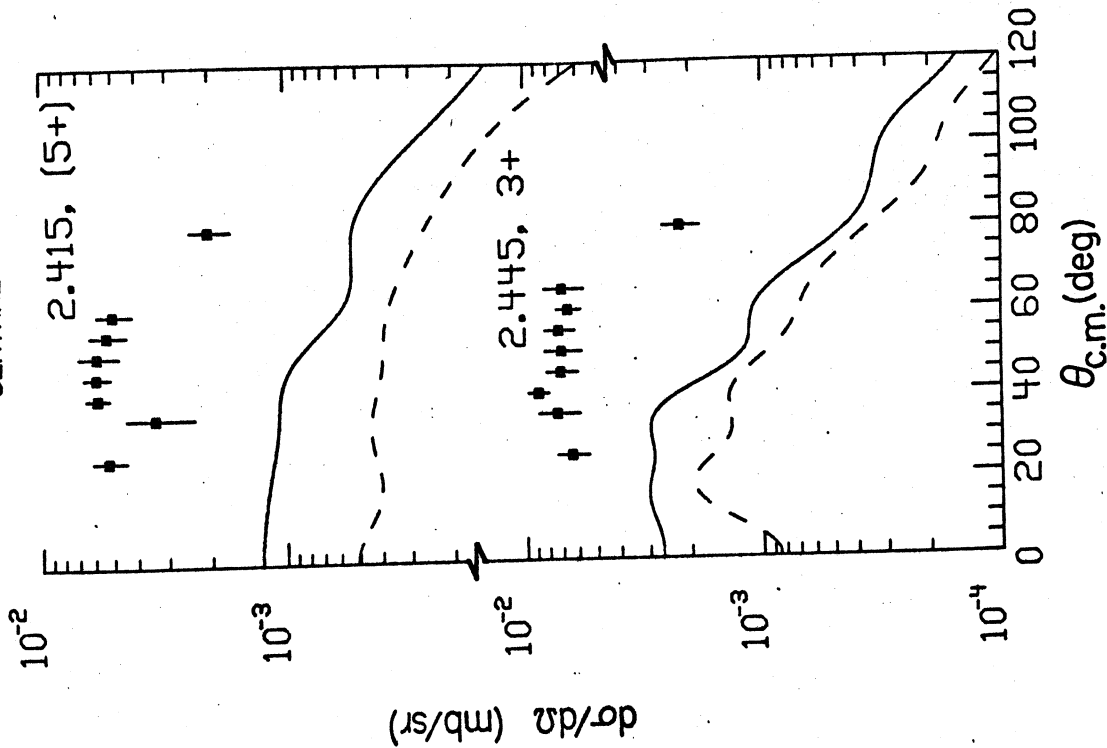
2+	3.33	3.35	3.36	3+	3.38	2+	3.34	3.37
4+	3.27	3.29	3.29	5+	3.29	1+	3.25	3.28
5+	3.22	3.24	3.26	6+	3.23	2+	3.16	
6+	3.17	3.19	3.20	3+	3.12	4+	3.05	
7+	3.12	3.13		4+	3.05	3+	2.99	
8+	3.06			2+	2.99	4+	2.93	
0+	2.92	2.93	2.96	1+	2.90	3+	2.88	
1+	2.89	2.85		5+	2.83	4+	2.78	
2+	2.82			4+	2.64	2+	2.64	
3+	2.50	2.60		1+	2.57	4+	2.56	2.58
4+	2.53	2.51		3+	2.42	5+	2.41	2.44
5+	2.48			4+	2.37	4+	2.31	
6+	2.40	2.41		2+	2.23	6+	2.20	2.22
7+	2.35	2.31		6+	2.18	5+	2.09	
0+	2.31			8+	1.92	4+	1.90	
1+	1.94			4+	1.79	2+	1.44	
2+	1.89			2+	1.41			
3+	1.51							

0+	1.51	0+	1.41	0+	1.44
138B <sub>A</sub> INTERACTION		138B <sub>A</sub> INTERACTION		EXPERIMENT	
138B <sub>A</sub>		138B <sub>A</sub>		138B <sub>A</sub>	





— CENTRAL+TENSOR+LS  
 - - - CENTRAL ONLY



— A = 136-140  
 - - - A = 136-145

— A = 136-140  
 - - - A = 136-145

